Transmission System and Microgrid Co-optimization Model

1. Introduction

The future power systems rely on moving towards a resilient and decentralized system accommodating a variety of supply and demand side technologies such as renewables and energy storages [**?**], MGs will play a critical role in this evolution by encouraging distributed local generation, autonomous operation in the case of transmission faults and enabling multiple future grid technologies. In addition, MGs could also alleviate transmission congestion, reduce transmission losses, and provide DR (DR)[**?**]. These characteristics make MGs a basic building block of a decentralized and robust future grid. With the possibility of numerous MG connected to the TS, the way the power systems operate will change dramatically. As each MG could be view as an independent entity with its own distributed generation, load and many other facilities such as energy storage and renewables depending on the MG's particular configuration. Each MG will have its own operation objective which could conflict with the TS's. A proper way to co-optimize the two systems will thus become very important for the efficient operation of the whole system in the future.

The co-optimization of TS and MG operation is a relatively new area. What has been done falls into two categories. One category [**? ? ? ? ? ? ? ?**] focuses on the optimization of MG operation with an abstract model for the TS. Specifically, those models model the TS as a node which connects to the MG and could buy or sell certain amount of energy from or to the MG at fixed prices. The elimination of the TS details makes such models less realistic as the nodal energy exchange and price information is based on the detailed model and can change over time. As a result, those models make the optimization of the MG less realistic and are unable to reflect MG's impact on the TS. The other category [**? ? ? ? ? ? ? ?**] focuses on the TS details with an over-simplified model for the MG. In those work, MGs are normally modeled as distributed generations (DG) which could only sell energy. In reality, a MG model could not only sell energy, but also buy energy from the TS, store energy, vary its load consumption (ie: providing DR). Therefore, MGs often have their own energy management systems and should ideally be modeled as a separate optimization problem. Treating MGs as DGs

once again fails to capture realistic impact of MGs on the TS and does not provide any insights of the influence of TS over the MG's internal operation. In the future where there will very likely be many MGs connected to the TS, the drawbacks of the above two modeling approaches will make themselves less and less applicable. In addition, the impact of DR on the TS could not be effectively studied with those two approaches as DR happens at the distribution level and requires a detailed model for the distribution side.

In this work, the operation of the TS and MG are optimized at the same time with a detailed model for each. A bilevel optimization approach is applied for this framework. Bilevel optimization is defined as a mathematical optimization problem in which one optimization problem (upper level problem) contains another optimization problem (lower level problem) [**?**]. There has been extensive study on bilevel optimization. There are two categories of approaches to solve bilevel optimization problems. The first category applies classical methods including single-level reduction [**?** **?**], descent methods [**?** **?**], penalty function methods [**?** **?**], and trust-region methods [**?** **?**]. Those methods are usually for problems with well-behaved properties such as linear, quadratic or convex functions, continuous differentiability and lower semi-continuity. Of those methods, the single level reduction method is the most widely used one when the lower level problem is convex and sufficiently regular. The single level reduction method is applied in this work. The second category applies evolutionary methods including genetic algorithms [**?**], particle swarm optimization [**?**], differential evolution [**?**], and metamodeling-based methods [**?**]. Those methods could tackle problem with fewer well-behaved properties mentioned above. However, they normally require much more computational efforts and do not provide performance guarantee. For a detailed review of different bilevel optimization methods, please refer to [**?** **?**].

In this work, the TS and the MG both are equipped with detailed models and comprehensive constraints. The TS model has a network with power flow constraints as well as renewable generation. To manage with the uncertainty in the renewable generation, the generator reserves in the TS as well as DR in the MG are used. One innovation of this work is that the DR is totally decoupled from the TS and is entirely modeled at the distribution system level MG. This is more realistic than common DR modeling at the transmission level. Bilevel optimization technique is used to co-optimize the two system, which gives a global optimal solution in terms of the operation schedules of the two systems in a single round of solving. In this optimization framework, the factors that affect the renewable (ie: wind in this study) penetration level in the TS

and the operation cost of the two systems are analyzed in details. Recommendations on how to improve the wind penetration level and reduce the system operation cost are given.The key contribution sof this work are summarized below:

(1) Bilevel optimization framework is proposed for the co-optimization of TS and MG.
(2) A detailed TS model with network and detailed MG model are for the first time applied in the cooptimization framework.
(3) DR is decoupled from the TS level and modeled at the distribution level, which provides a more realistic optimization model.
(4) Factors that affect the system wind penetration level and operation cost are reviewed.
(5) Recommendations are given to maximize the wind penetration and reduce the system operation cost.

The structure of the paper is as follows; the bilevel optimization model is discussed in section **??**. Numerical results for are reported in Section3. Concluding remarks and future research directions are given in Section 4.

2. Optimization Model

In this section, the structure of the bi-level optimization problem is described. The general formulation of a bilevel optimization is given below:

$$
\begin{aligned}
&\min_{x\in X, y\in Y} F(x,y) \\
\text{st: } &G_i(x,y) \leq 0, \text{for } i \in \{1,2,...,I\} \\
&H_k(x,y) = 0, \text{for } k \in \{1,2,...,K\} \\
&y \in \underset{y\in Y}{\operatorname{argmin}}\{f(x,y) : g_j(x,y) \leq 0, \text{for } j \in \{1,2,...,J\}, \\
&h_m(x,y) = 0, \text{for } m \in \{1,2,...,M\}\}
\end{aligned}
$$

In the above formulation, $x, F(x,y), (G_i, H_k)$ are the optimization variables, objective function and constraints of the upper level problem. Whereas, $y, f(x,y), (g_i, h_m)$ are the optimization variables, objective function and constraints of the lower level problem. According to this formulation, the bilevel formulation of the TS and MG co-optimization is given in the following sections.

2.1. Upper Level Problem: TS Unit Commitment Problem

In this study, we try to increase the renewable penetration level (eg: wind) in the TS to cater the green energy requirement for the near future. The uncertainty introduced by the renewable forecast needs to be compensated by the TS generator's reserve as well as the DR from the MG. The upper level transmission day-ahead unit commitment problem seeks to compute the optimal operation schedule including the generator commitment status $w_{g,t}$, the generation output $P_{g,t}$, upward and downward generator's reserve $R^{up}_{g,t}$, $R^{dn}_{g,t}$, and MG DR price $P^{dr}_{g,t}$ to minimize the total TS operation cost. The optimization variables are denoted by the vector x_t, and include:

$$x_t = [W_{g,t}, P_{g,t}, R^{up}_{g,t}, R^{dn}_{g,t}, P^{dr}_t]$$

The objective of the upper level optimization problem is to minimize the TS operation cost including the generator commitment cost, generation cost, reserve cost, energy exchange cost with the MG and the MG DR cost.

Objective function:

$$\begin{aligned} F(\{x_t\}_{t=1}^T) &= \textstyle\sum_{t=1}^{T}\sum_{g=1}^{G}(C^c_{g,t}W_{g,t} + C_{g,t}P_{g,t} + C^r_g(R^{up}_{g,t} + R^{dn}_{g,t}) \\ &- P^{im}_t C^{im}_t + P^{ex}_t C^{ex}_t \\ &+ P^{dr}_t(DR^{up}_t + DR^{dn}_t)) \end{aligned}$$

The constraints of the TS are listed below.

Power flow constraints:

$$-Line \leq GSF * Pinj_t \leq Line, t \in 1, ..., T \quad (1)$$

$$-Line \leq GSF * Pinj^*_t \leq Line, t \in 1, ..., T \quad (2)$$

$P_{inj,t}$ is the DC net power injection vector (ie: generation + wind - demand) for all the buses in each hour. $P^*_{inj,t}$ incorporates the wind forecast error, generator reserve and MG DR on top of $P_{inj,t}$. Eqn (1),(2) bounds the transmission line flows within the flow limits.

Generator constraints:

$$\underline{P}_g \leq P_{g,t} \leq \overline{P}_g, t \in 1, ..., T \quad (3)$$

$$(P_{g,t} + R^{up}_{g,t}) - (P_{g,t-1} - R^{dn}_{g,t-1}) \leq \overline{R}_g, t \in 2, ..., T \quad (4)$$

$$\underline{R}_g \leq (P_{g,t} - R^{dn}_{g,t}) - (P_{g,t-1} + R^{up}_{g,t-1}), t \in 2, ..., T \quad (5)$$

Eqn (3) bounds the generator generation within its capacities. Eqn (4),(5) satisfies the generator ramping capability.

Power balance constraint:

$$\sum_{g=1}^{G} P_{g,t} + \mathbf{1}_{1\times N_b} * L_t + W^f = P_t^{im} - P_t^{ex}, , t \in 1, ..., T \tag{6}$$

where $\mathbf{1}_{1\times N_b}$ is a all ones vector of length N_b. The dot product $\mathbf{1}_{1\times N_b} * L_t$ gives the total load in the system. Eqn (6) keeps the total system generation the same as the total system load.

Reserve constraints:

$$W_t^{up} <= DR_t^{up} + \sum_{g=1}^{G} R_{g,t}^{dn}, t \in 1, ..., T \tag{7}$$

$$W_t^{dn} <= DR_t^{dn} + \sum_{g=1}^{G} R_{g,t}^{up}, t \in 1, ..., T \tag{8}$$

W_t^{up} is deviation between the wind forecast and the scenario with the largest wind generation, and could be compensated by less generation of the transmission generators (ie: R_t^{dn}) or more consumption of the MG dispachable load (ie: DR_t^{up}). W_t^{dn} is deviation between the wind forecast and the scenario with the smallest wind generation, and could be compensated by more generation of the transmission generators (ie: R_t^{up}) or less consumption of the MG dispachable load (ie: DR_t^{dn}). Eqn (7), (8) ensure enough generator reserve and MG DR to compensate the possible wind forecast deviation.

DR price constraint:

$$P_t^{dr} >= P_t^{d}, t \in 1, ..., T \tag{9}$$

As demand response could change the original demand profile and consequently cause some inconvenience to the consumers, a penalty term could be used as a lower price cap for the DR to account for that, which is reflected by Eqn (9).

Finally, the TS unit commitment problem is formulated as:

$$\begin{aligned} &\min_{\{x_t\}_{t=1}^{T}} F\left(\{x_t\}_{t=1}^{T}\right) \\ &\quad \text{s.t. } (1) - (10) \\ &\qquad \mathbb{P}(eqn(2,4,5,7,8)) \geq 1 - \epsilon \end{aligned}$$

A chance-constrained approach is applied here for the stochastic equations (2,4,5,7,8) as [**?**] shows that a chance-constrained approach strikes a good balance between the system cost, reliability and wind penetration. The chance constraints in this study are required to meet the specified probability level 1 - ϵ jointly. It is also possible to write individual chance constraints, where each constraint i is required to meet a specified

probability level 1 - ϵ_i individually. In the latter case, different i can be selected for each constraint allowing critical constraints or time periods to be managed in a robust way, with increased flexibility elsewhere. Interested readers could refer to [**?**] for a detailed explanation of the chance-constrained approach.

2.2. Lower Level Problem: MG Operation Optimization

A comprehensive MG is considered in this work. The MG consists of distributed generation (DG), a storage unit, aggregated dispatchable and non-dispatchable loads, and is able to exchange power with the main grid. Since a MG typically covers a small local area with very limited power capacity, it thus has very limited influence in the setting of the market price, it is assumed that the MG is a price taker in the problem formulation. The goal of the MG optimal dispatch model is to compute the generation schedule $P^m_{g,t}$, the battery energy state B_t, the battery charging and discharging decision Pb_t, MG energy import P^{im}_t and export P^{ex}_t schedule, dispatchable load profile L^d_t and the upward/downward DR^{up}_t, DR^{dn}_t provided by the dispachable load. The lower level optimization variables are denoted by the vector y_t, and include:

$$y_t = [P^m_{g,t}, B_t, P^{im}_t, P^{ex}_t, DR^{up}_t, DR^{dn}_t, L^d_t]$$

The objective of the MG optimization is to minimize the MG operation cost including its generation cost, battery maintenance cost, energy exchange cost with the TS and maximize its dispatchable load utility and DR revenue.

Objective function:

$$f(\{y_t\}^T_{t=1}) = \sum_{t=1}^{T}(C^m_g P^m_{g,t} + C^b B_t + P^{im}_t C^{im}_t - P^{ex}_t C^{ex}_t - C^d_t L^d_t - P^{dr}_t (DR^{up}_t + DR^{dn}_t))$$

The constraints for the MG are given below. The λ and μ variables next to the constraints are the dual variables associated with the corresponding inequality and equality constraints.

Generator constraints:

$$\underline{P}^m \leq P^m_{g,t} \leq \overline{P}^m, \lambda 1_t, \lambda 2_t, t \in 1, ..., T \tag{11}$$

Eqn (11) limits the generator's output within the upper and lower bound.

Dispatchable load constraint:

$$\underline{L}^d_t \leq L^d_t \leq \overline{L}^d_t, \lambda 3_t, \lambda 4_t, t \in 1, ..., T \tag{12}$$

Eqn (12) shows that the dispatchable loads need to stay within predefined bounds. The room between the dispatchable load set point and the bounds could be used as DR to compensate for wind forecast errors.

DR constraints:

$$L_t^d + DR_t^{up} \leq \overline{L}_t^d, \lambda 5_t, t \in 1, ..., T \tag{13}$$

$$Ld_t - DR_t^{dn} \geq \underline{L}_t^d, \lambda 6_t, t \in 1, ..., T \tag{14}$$

$$0 \leq DR_t^{up} \leq W^{up}, \lambda 7_t, \lambda 8_t, t \in 1, ..., T \tag{15}$$

$$0 \leq DR_t^{dn} \leq W^{dn}, \lambda 9_t, \lambda 10_t, t \in 1, ..., T \tag{16}$$

Eqn (13), (14) limit the DR of dispatchable load within the dispatachable load bounds. Also the amount of DR could not exceed the wind forecast deviation, which is reflected by Eqn (15), (16).

Storage constraints:

$$\underline{P}^b \leq P_t^b \leq \overline{P}^b, \lambda 11_t, \lambda 12_t, t \in 1, ..., T \tag{17}$$

$$\underline{B} \leq B_t \leq \overline{B}, \lambda 13_t, \lambda 14_t, t \in 1, ..., T \tag{18}$$

$$B_t = B_{t-1} + P_{t-1}^b, \mu 1_t, t \in 1, ..., T \tag{19}$$

Equations (17) and (18) restrict the storage's output power and the energy state to their upper and lower bounds. Equation (19) shows the transition of the storage energy state from one period to the next. A positive/negative P_t^b value corresponds to charging/discharging of the battery.

Import and Export constraints:

$$0 \leq P_t^{im}, \lambda 15_t, t \in 1, ..., T \tag{20}$$

$$0 \leq P_t^{ex}, \lambda 16_t, t \in 1, ..., T \tag{21}$$

The MG import and export power is defined to be non-negative as shown in Eqn (20), (21).

Power balance constraint:

$$P_t^m - P_t^b - L_t^i - L_t^d = P_t^{ex} - P_t^{im}, \mu 2_t, t \in 1, ..., T \tag{22}$$

Eqn (22) requires the MG load to be met with different power sources.

Finally, the MG optimal dispatch can be formulated as:

$$\min_{\{y_t\}_{t=1}^T} f\left(\{y_t\}_{t=1}^T\right)$$
$$\text{s.t. } (12) - (25)$$

The interactions between the TS and MG is illustrated in Fig. 1

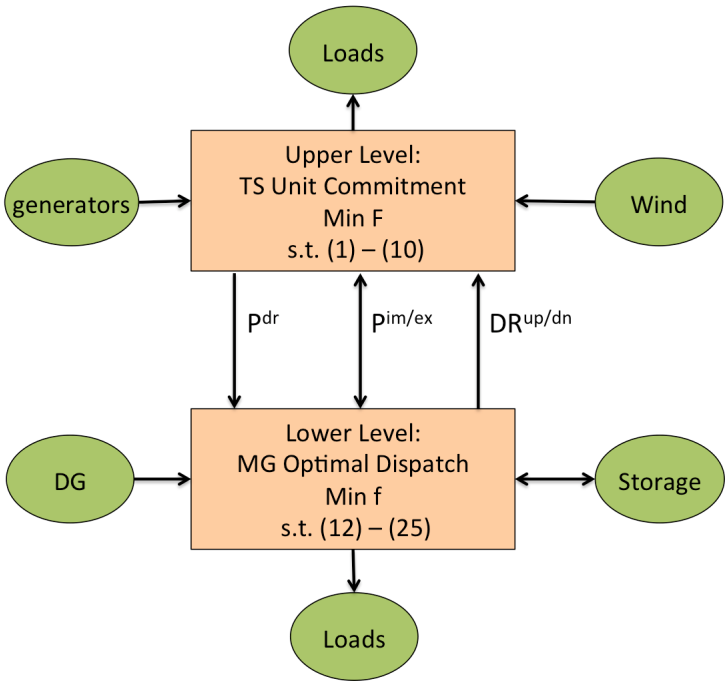

Figure 1: Interactions between the TS and MG

2.3. Reformulation to a Single Level Problem

When the lower level problem is convex and satisfies certain regularity conditions, it can be replaced by its Karush-Kuhn-Tucker(KKT) conditions [**?**], yielding a single -level problem reformulation as below:

$$\min_{x\in X, y\in Y} F(x,y)$$

st: $G_i(x,y) \leq 0, \text{for } i \in \{1,2,...,I\}$

$H_k(x,y) \leq 0, \text{for } k \in \{1,2,...,K\}$

$g_i(x,y) \leq 0, \text{for } i \in \{1,2,...,j\}$

$h_m(x,y) \leq 0, \text{for } m \in \{1,2,...,M\}$

dual feasibility: $\lambda_i \geq 0, \text{for } i \in \{1,2,...,j\}$

complementary slackness: $\lambda_i * g_i(x,y) = 0, \text{for } i \in \{1,2,...,j\}$

stationarity: $\nabla L(x,y,\lambda,\mu) = 0$

where :

$$L(x,y,\lambda) = f(x,y) + \sum_{i=1}^{J} \lambda_i * g_i(x,y) + \sum_{m=1}^{M} \mu_m * h_m(x,y)$$

The lower level problem in this study is a linear program and could thus be replaced by its KKT conditions. The KKT conditions are given below:

Stationarity:

$$C^m + \lambda 2_t - \lambda 1_t + \mu 2_t = 0 \tag{24}$$

$$-C^d - \lambda 4_t + \lambda 3_t - \mu 2_t = 0 \tag{25}$$

$$C^b + \lambda 13_t - \lambda 14_t + \mu 1_t = 0 \tag{26}$$

$$C_t^{im} - \lambda 14_t - \mu 2_t = 0 \tag{27}$$

$$-C_t^{ex} - \lambda 15_t + \mu 2_t = 0 \tag{28}$$

$$\lambda 8_t - \lambda 11_t - \mu 1_t - \mu 2_t = 0 \tag{29}$$

$$-P_t^{dr} - \lambda 8_t - \lambda 7_t + \lambda 5_t = 0 \tag{30}$$

$$-P_t^{dr} - \lambda 10_t - \lambda 9_t + \lambda 6_t = 0 \tag{31}$$

Dual feasibility:

$$\lambda 1 ... \lambda 16 \geq 0 \tag{32}$$

Complementary slackness:

$$\lambda 1_t * (P_t^m - \underline{P}^m) = 0 \tag{33}$$

$$\lambda 2_t * (P_t^m - \overline{P}^m) = 0 \tag{34}$$

$$\lambda 3_t * (L_t^d - \overline{L}_t^d) = 0 \tag{35}$$

$$\lambda 4_t * (L_t^d - \underline{L}_t^d) = 0 \tag{36}$$

$$\lambda 5_t * (DR_t^{up} + L_t^d - \overline{L}_t^d) = 0 \tag{37}$$

$$\lambda 6_t * (-DR_t^{dn} - L_t^d + \underline{L}_t^d) = 0 \tag{38}$$

$$\lambda 7_t * (DR_t^{up}) = 0 \tag{39}$$

$$\lambda 8_t * (DR_t^{up} - W^{up}) = 0 \tag{40}$$

$$\lambda 9_t * (DR_t^{dn}) = 0 \tag{41}$$

$$\lambda 10_t * (DR_t^{dn} - W^{dn}) = 0 \tag{42}$$

$$\lambda 11_t * (P_t^b - \overline{P}_t^b) = 0 \tag{43}$$

$$\lambda 12_t * (P_t^b - \underline{P}_t^b) = 0 \tag{44}$$

$$\lambda 13_t * (B_t - \overline{B}) = 0 \tag{45}$$

$$\lambda 14_t * (B_t - \underline{B}) = 0 \tag{46}$$

$$\lambda 15_t * (B_t) = 0 \tag{47}$$

$$\lambda 16_t * (B_t) = 0 \tag{48}$$

The reformulated single level problem has the following format:

$$\min_{\{x_t, y_t, \lambda_t, \mu_t\}_{t=1}^{T}} F\left(\{x_t, y_t, \lambda_t, \mu_t\}_{t=1}^{T}\right)$$
$$\text{st: } (1) - (50)$$

This reformulation is not easy to solve mainly due to the non-convexity in the complementary slackness and bilinear terms in the objective function. The big-M reformulation is used to transform the complementary conditions to mixed integer constraints. The Mccormick Envelope technique is applied to change the bilinear term into a single variable with additional linear constraints. The technical details of those two methods are given in the appendix.

With the big-M reformulation and Mccormick envelope methods, a set of binary variables and additional constants are introduced. The bilevel problem becomes a single level becomes mixed integer linear problem and could thus be solved with a wide range of commercial solvers such as Cplex and Gurobi.

3. Numerical Results

In this section, the transmission model described in Section 2 is applied to the IEEE 30-bus system, shown in Figure 2. Interested readers are referred to [**?**] for detailed parameters of the TS. The parameters of the 25 MW MG is listed in the Appendix. Multiple wind farms are positioned at different buses in the TS to provide renewable generation. A comprehensive MG is considered in this work. The MG consists of a generator, a storage unit, DL and non-DL, and is able to operate in islanded mode and grid-connected mode. The parameter values of the 25 MW MG are listed in the appendix.

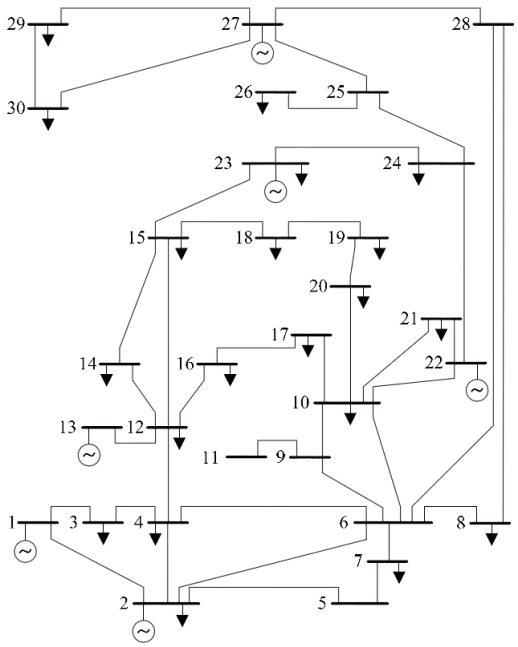

Figure 2: IEEE 30 Bus System

The wind data for the wind farms in the TS are selected from the NREL-Eastern Wind Integration Study dataset [**?**]. Using three years of data, 24-hour trajectories are grouped to identify a set of similar trajectories, with a common initial condition. The set contained 54 trajectories and were used to represent the realizations of a similar forecast. The central trajectory of the group was selected as the wind forecast, and the remaining were used to estimate the distribution of forecast errors, as described in [**?**]. From the forecast error distribution, 10000 scenarios are used to generate a robust wind error scenario set.

For the MG import price, the locational marginal price for each buse in the TS without the MG is precomputed for a wide range of loading conditions. Then a first order equation is fitted between the price and the import quantity. This way the import price is approximated as a linear function of the import quantity as below:

$$C_t^{im} = a * P_t^{im} + b \tag{50a}$$

where a and b are two constants representing the slope and intercept of the pricing equation. The method enables a dynamic pricing scheme which accounts for varying system loading conditions and at the same time preserves the convexity of the problem. The export price is defined as 90% of the import price at each quantity to avoid the market flaw of buying energy and selling back to make money. This pricing scheme

might not be the best pricing scheme. The optimal pricing scheme is out of the focus and scope of the work.

The objective of this work is to analyze different factors that affect the WP in the TS and the operational cost of the two systems in this co-optimization framework as well as the standalone framework. To this end, this section is divided into a WP result part and system cost part.

3.1. WP Results

The definition of WP is based on the wind power capacity penetration defined by the European Wind Energy Association [**?**]. It is the ratio of the installed wind capacity divided by the peak system load.

3.1.1. Location of Wind in the System

To generate some benchmarks, a wind farm is positioned at different buses in the TS with no MG. The maximum WP in each case is recorded. The results for some representative bus are given in Tab.1.

Wind Bus	Max WP	Reason
5	38%	Reach transmission limit
8	28%	Use up generator reserve
15	38%	Use up generator reserve
30	28%	Reach transmission limit
8 and 30	38%	Use up generator reserve

Table 1: WP at different buses

As the TS has a network with limits on transmission lines, different buses have different capacities in terms of renewable injection. Table 1 shows that bus 8 and 30 allows smaller WPs compared to bus 5 and 15 as bus 8 and 30 are connected to transmission lines with smaller capacity. For bus 5 and 15, the connected line capacity is large enough to use up the generator reserve to achieve maximum WP. The case with two wind farms at bus 8 and 30 demonstrates that the system is more likely to use up the generator reserves for maximum WP if there are multiple wind farms at different locations in the system as the generator's reserve is less likely to be constrained by line limits in this case. The method to find buses that are more prone to violate transmission constraints in given in [**?**]. As a result, wind farms should be placed on buses with

generous transmission capacity and possibly at multiple locations to achieve high level of WP.

3.1.2. WP with a MG

To illustrate the effects of MG on the WP, a 25MW MG with 50% DL is connected to the wind buses in the previous section. Here the DL percentage is defined as the ratio of the maximum DL and the sum of maximum DL and non-dispatchable load. The size of the MG (25MW in this case) is with regards to the generation capacity of the MG. The WP with and without the MG is given in Fig.3.

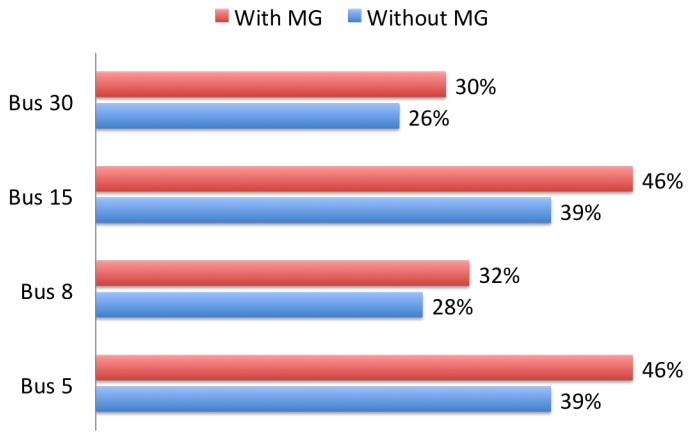

Figure 3: WP with and without MG at different buses

Fig.3 illustrates that the WP in general increases since the DR provided by the MG could act as reserve and locally offset some wind forecast error at the wind bus. The penetration increase for bus 8 and 30 is less than that of bus 5 and 15 as bus 8 and 30 are subject to tighter transmission line limits. Tab. 2 shows the the maximum WP when the MG is placed at different buses from the wind farm bus. This table shows that when the MG and wind farm are at different buses, the WP level could only be less than that when they are at the same bus as the later case could bypass transmission constraints and directly offset wind forecast error, which is not possible for the former case.

Wind Bus	MG Bus	Max WP
5	8	45%
5	15	45%
5	30	45%
8	5	28%
8	15	28%
8	30	28%

Table 2: WP with the wind farm and MG at different buses

3.1.3. WP for different MG sizes and DL levels

As the amount of reserve is proportional to the size of the MG and the amount of DL in the MG, the WP with regards to those two factors are analyzed here. To simulate a MG with varying sizes, the MG parameters except for the ones related to the costs are scaled by the same constant. The wind farm and MG are both located at bus 5 to guarantee enough line capacity and no interference from line constraints. Fig. 4 shows WPs for different sizes of a MG with 50% of the loads being dispachable. Fig. 5 shows WPs for a 25MW MG with different levels of DLs. It can been seen from the two figures that WPs are linearly proportional to MG size and DL levels as there is more MG DR to offset the wind forecast error.

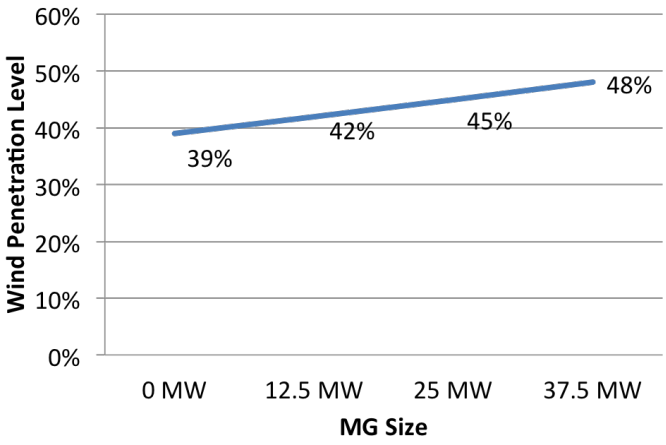

Figure 4: WP for different MG sizes

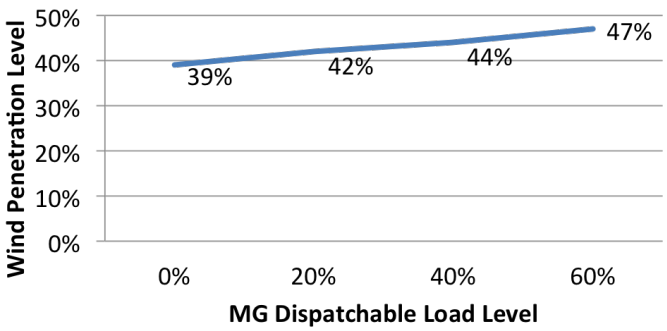

Figure 5: WP for different DL levels

3.2. System Cost Results

One goal of the TS and MG co-optimization is to reduce the individual system's operation cost. Different factors that affect the cost of the two systems are explored in this section. For the figures in this subsection, SA stands for standalone mode, while COOP stands for co-optimization mode. In the COOP mode, the MG is able to provide DR as reserve to account for the wind forecast error in the TS and exchange energy with the TS. In the SA mode, the MG is separated from the TS and thus could not exchange energy with the TS or provide any DR.

3.2.1. WP on transmission and MG cost

As WP is a key concern of the future grid and also a focus of this study, the WP is varied to see the impact on the TS and MG cost. A 25MW MG with 50% DL is connected to bus 5 which also connects the wind farm. The results are displayed in Fig. 6.

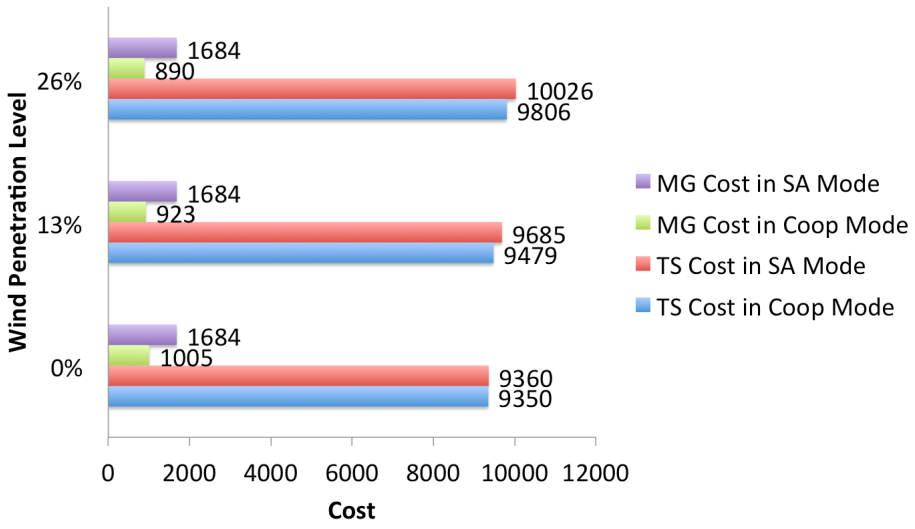

Figure 6: TS cost for different WP levels

From Fig. 6, when the WP increases from 0 to 13%, the TS cost in the co-optimization mode increases slightly as most of the wind forecast error is accounted by MG DR, consequently the MG operation cost decreases a lot due to the revenue from DR. As the WP is further increased, the transmission cost starts to significantly increase as the DR capacity is used up and the expensive generator reserve is put in use. On average the reserve cost drops by 25% in the co-optimization mode for 13% and 26% wind penetration.The MG decreases slightly as it could not provide much DR for a bigger WP. The operational costs of the two systems are once again smaller in the co-optimization mode for the same reason. In the SA mode, the MG cost is the same for all three cases as the MG configuration stays the same for all of them.

3.2.2. MG size on transmission cost

The TS is optimized with different sizes of MG connected to bus 5 and the operation cost is reported in Fig. 7. For all the cases, the DL level in the MG is 50%. The wind farm is connected to bus 8, and a fixed 10% WP is used.

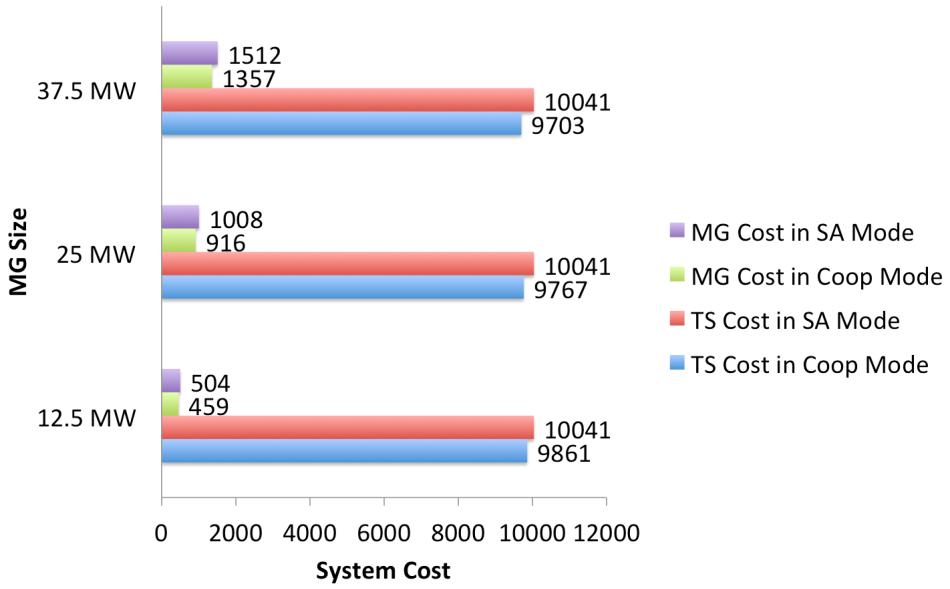

Figure 7: TS cost for different MG sizes

From Fig. 7, it can be seen that in the co-optimization mode the cost of the TS decreases with the increase in MG size. The main reason behind is the use of the cheaper MG DR to compensate the wind deviation instead of using the expensive generator's reserve. In addition, the individual system's cost is always smaller in the co-optimization mode compared to the standalone mode as both systems have opportunities to arbitrage in the energy exchange transactions in addition to the benefits from the reserve provision. In the SA mode, the TS cost is the same for all three cases as the TS configuration stays the same for all of them.

3.2.3. MG DL level on transmission and MG cost

For the setting of a 25MW MG and 10% WP at bus 5 in the TS, the TS and MG operation cost at different levels of MG DL are reported in Fig. 8.

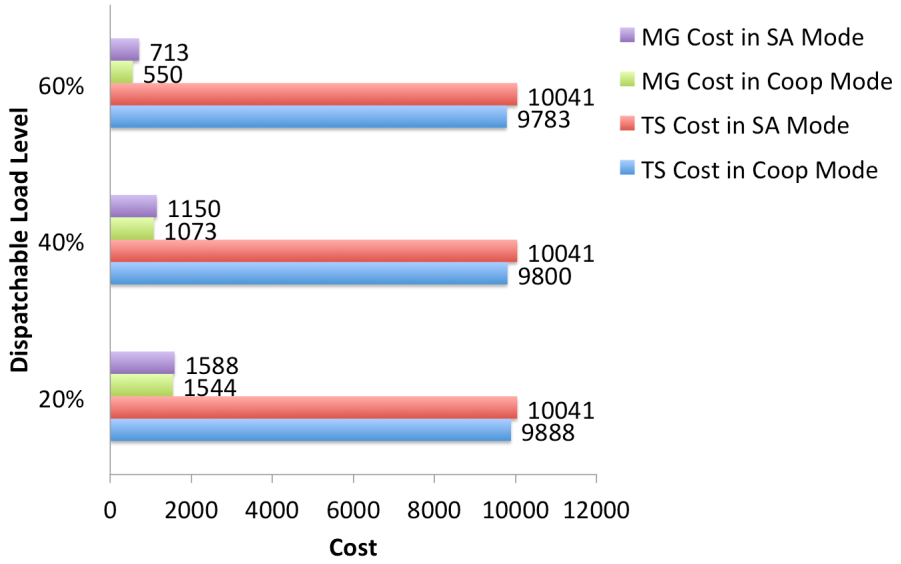

Figure 8: TS cost for different MG DL levels

It is shown in Fig.8 that the TS cost decreases with an increasing DL level as more wind forecast error is accounted by the cheaper MG DR. Similarly, the MG cost decreases with the increasing DL level as the MG has more DR to sell. Once again, the co-optimization framework enables mutual financial benefits from the reserve service and energy exchange and thus reduces the cost of the two systems.

3.2.4. Wind farm and MG locations on transmission and MG cost

With 10% WP, a 25MW MG with 50% DL system configuration, the location of the wind farm and the MG does not make a difference in terms of the system operation cost as this WP does not cause congestion anywhere in the system. However it is possible that a higher WP at certain buses could cause congestion and significantly increases the system operating cost, which is a well-known fact in the power systems. The way to wisely position the MG to deal with the congestion and reduce the system cost is discussed in **??**.

4. Concluding Remarks

This paper presents an analysis of a grid-connected microgrid with DR and distributed generation.

Acknowledgements

This material is based upon work supported by the US Department of Energy under Award Number DE-OE0000843. Disclaimer: This report was prepared as an account of work sponsored by an agency of the United States Government. Neither the United States Government nor any agency thereof, nor any of their employees, makes any warranty, express or implied, or assumes any legal liability or responsibility for the accuracy, completeness, or usefulness of any information, apparatus, product, or process disclosed, or represents that its use would not infringe privately owned rights. Reference herein to any specific commercial product, process, or service by trade name, trademark, manufacturer, or otherwise does not necessarily constitute or imply its endorsement, recommendation, or favoring by the United States Government or any agency thereof. The views and opinions of authors expressed herein do not necessarily state or reflect those of the United States Government or any agency thereof.

5. Appendix

5.1. Big-M Method

The complementary conditions are set of constraints with the following format:

$$\lambda_i * g_i(x, y) = 0$$

Specifically, given a sufficiently large positive value M_i and binary value ϕ_i, the complementary conditions could be reformulated as below:

$$-(1 - \phi_i) * M_i \leq g_i(x, y)$$
$$\lambda_i \leq \phi_i * M_i$$

For a detailed treatment of the Big-M method, please refer to [**?**].

5.2. Mccormick Envelope

For a toy optimization problem of the following format:

$$\min Z = x * y \tag{51}$$
$$\underline{x} \leq x \leq \overline{x}$$
$$\underline{y} \leq y \leq \overline{y}$$

The problem could be reformulated by introducing a new variable $w = x * y$ as follow:

$$\begin{aligned} \min\ Z &= w \qquad (52)\\ w &\geq \overline{x} * y + x * \overline{y} - \overline{x} * \overline{y}\\ w &\geq \underline{x} * y + x * \underline{y} - \underline{x} * \underline{y}\\ w &\leq \overline{x} * y + x * \underline{y} - \overline{x} * \underline{y}\\ w &\leq \underline{x} * y + x * \overline{y} - \underline{x} * \overline{y}\\ \underline{x} &\leq x \leq \overline{x}\\ \underline{y} &\leq y \leq \overline{y} \end{aligned}$$

For a detailed treatment of the Big-M method, please refer to [**?**].

5.3. Microgrid Parameters

The parameter values for a 25 MW MG are listed in the table below.

Parameters	Values
$\underline{L}_t^d$	6.6MW
$\overline{L}_t^d$	12MW
L_t^i	12MW
$\overline{B}$	10MW
$\underline{B}$	0MW
C^b	\$0.1/MW
C_t^m	\$3.5/MW
C_t^d	\$3.55/MW
$\overline{P}_t^d$	\$1/MW
$\overline{P}^m$	25MW
$\underline{P}^m$	0MW
$\underline{P}^b$	-5MW
$\overline{P}^b$	5MW

Table 3: MG parameter values

6. References